

Research Paper

Enhancing Seismic Performance of Steel Bridge Piers with Rocking Mechanism and Friction Damper: A Finite Element Simulation Study

Mohammad Hossein Mahmoudi¹ and Akbar Vasseghi^{2*}

1. Ph.D. Student, International Institute of Earthquake Engineering and Seismology (IIEES), Tehran, Iran
2. Associate Professor, Structural Engineering Research Center, International Institute of Earthquake Engineering and Seismology (IIEES), Tehran, Iran,
*Corresponding Author; email: vasseghi@iiees.ac.ir

Received: 26/10/2023

Revised: 02/02/2024

Accepted: 17/02/2024

ABSTRACT

This paper presents a novel rocking system for bridge piers that aims to minimize structural damage and reduce residual drift during seismic events. This system relies on gravity for re-centering and does not utilize post-tensioned tendons. It consists of a pair of tubular steel columns attached to the foundation and cap beam with rocking connections. Each connection utilizes a friction damper that absorbs energy through friction at low lateral displacement and plastic deformation at large lateral displacement. Finite element (FE) simulation was utilized to evaluate the behavior of this system under vertical and lateral loading. The finite element models under two different gravity loads were subjected to lateral cyclic loading to study the re-centering characteristics of the system. The analyses have demonstrated that the system exhibits a flag-shaped hysteresis response with minimal residual drift. A supplementary analysis has also shown that any residual drift in this system can be recovered by loosening bolts in the frictional connection

Keywords:

Bridge pier; Tubular steel column; Rocking system; Self-centering; Finite element analysis (FEA)

1. Introduction

The integration of performance-based earthquake engineering principles into conventional design practices has highlighted the significance of structural damage and residual deformation that can compromise a structure's functionality (Bozorgnia & Bertero, 2004). Recent research has focused on developing high-performance structural materials and systems that minimize damage and residual deformation (Ricles et al., 2002; Tremblay et al., 2008). One such system is the rocking system, which employs unbonded post-tensioned tendons to connect prefabricated structural elements. The gap created by the rocking mechanism at the connection interface

offers significant deformation capacity under lateral loading. The addition of energy-dissipating elements at rocking interfaces results in a hybrid system with a flag-shaped hysteresis curve. Structures with this type of mechanism will sway under lateral loads and return to their original positions with no significant damage.

Despite the incorporation of existing seismic regulations in conventional bridge design practices, recent seismic events have underscored the susceptibility of bridges to damage (Aydan, 2008; Elnashai et al., 2012). Even earthquakes of moderate intensity have the potential to induce extensive structural damage and potential bridge

failure, leading to significant societal consequences. This underscores the necessity for the development of bridge elements and systems with damage avoidance mechanisms. Moreover, the increasing interest in accelerated bridge construction (ABC) is geared towards alleviating traffic congestion and disruptions linked with on-site construction activities (Culmo et al., 2011). One approach to achieve these goals is to use rocking bridge piers, where prefabricated components could be assembled on-site rapidly.

This paper presents the results of a numerical study on a novel rocking system that was developed for bridge piers with tubular steel columns (Vasseghi & Mahmoudi, 2024). Finite element (FE) simulation was utilized to evaluate the behavior of the system under vertical and lateral loading. The finite element model was subjected to lateral cyclic loading under two different gravity loads in order to investigate the re-centering characteristics of the system.

2. Prior Research

The phenomenon of rocking behavior was initially investigated by Housner (Housner, 1963), following observations made during the Arvin-Tehachapi (1952) and Chilean (1960) earthquakes. It was observed that structures designed to rock unintentionally were able to survive, while more stable structures suffered severe damage. Research on the application of unbonded post-tensioned tendons in building and bridge components began in the mid-1990s, with studies by Cheok and Lew (Cheok & Lew, 1991) and Priestley and Tao (Priestley & Tao, 1993). These studies demonstrated that using unbonded tendons in pre-cast concrete beam-column connections led to less damage and residual displacement than reinforced cast-in-situ connections. Due to the crushing of beams on the outer edges caused by the rocking mechanism (Stone et al., 1995), steel elements have been proposed to reinforce the connection interface (Li et al., 2008; Rodgers et al., 2012). Post-tensioning was then extended to steel moment-resisting frames (Ricles et al., 2001), and different types of energy dissipators (EDs) such as bolted seat angles (Tremblay et al., 2008), buckling restrained steel bars (Christopoulos

et al., 2002; Guerrini et al., 2015), frictional energy-dissipating devices (Christopoulos et al., 2008; Wolski et al., 2009), and hourglass-shaped steel cylindrical pins (Vasdravellis et al., 2013) have been used to enhance the energy dissipation property of such systems. The same technique was applied to concrete bridge piers (Mander & Cheng, 1997), with researchers proposing the use of steel (Hewes, 2002; Thonstad et al., 2017) or fiber-reinforced plastic confinements (ElGawady & Sha'lan, 2011; White & Palermo, 2016), steel armored interface (Palermo et al., 2007; Solberg et al., 2009), and fiber-reinforced concrete (Billington & Yoon, 2004; Trono et al., 2015) to mitigate damage at the rocking interface.

Numerous studies have been conducted to improve the behavior of old and new steel bridge piers, as many of them were damaged during the 1995 Kobe earthquake in Japan (Bruneau et al., 1996). The Japan Design Specification of Highway Bridges (Association, 2002) was revised after extensive cyclic tests were carried out by the Public Works Research Institute of Japan (Nishikawa et al., 1996) on steel bridge columns with different configurations. MacRae and Kawashima (MacRae & Kawashima, 2001) tested 24 large-scale steel piers with stiffened hollow and concrete-filled sections, and found that such piers had deficiencies such as global or local buckling in hollow sections, and low deformation capacity in concrete-filled sections. Aoki and Susantha (Aoki & Susantha, 2005) investigated the effect of cross-sectional aspect ratios on the behavior of rectangular steel piers through experimental work, in which failure was described as progressive buckling at the base of all seven specimens. Failure due to local buckling has also been reported in linearly tapered (Susantha et al., 2006) and thick-walled steel bridge piers (Ge et al., 2013). Vasseghi (Vasseghi et al., 2021) conducted a study to explore the feasibility of implementing a rocking system for highway bridges in Iran. In this study, the seismic performances of the rocking system for three typical bridges in Iran were compared with those of the conventional system. The seismic response of each system was evaluated by nonlinear time history analyses using seven earthquake records. The results of

this study showed that the peak lateral drifts in the rocking system increased by less than 20%, but the residual drifts were reduced by more than 85%.

3. Description of the Rocking Bridge Pier

The bridge bent in this system comprises a precast cap beam, a pair of prefabricated tubular steel columns, and pocket-type rocking connections. Figure (1) shows cross-sectional views of a typical bridge bent with rocking connections in both normal and rocking states. The components of the rocking connection are shown in Figure (2). They include an embedded steel sleeve component designed to receive the column end, a center shear pin, and a ring plate bearing against the column and connected to the sleeve component by high-strength bolts. The boltholes in the ring plate are oversized to allow for sliding relative to the embedded sleeve component, thereby activating friction and energy dissipation across the contact surfaces.

Figure (3) shows the pocket-type connection in the rocking state. The bolts are pre-tensioned to provide a frictional connection for the ring plate and the embedded sleeve. During rocking, the

column pushes the ring plate to move relative to the embedded sleeve, activating energy dissipation through friction until the oversized holes on the ring plate bear against the bolts. At that point, the second level of energy dissipation occurs through the yielding of the ring plate material. Figure (4) shows the position of the ring plate relative to the

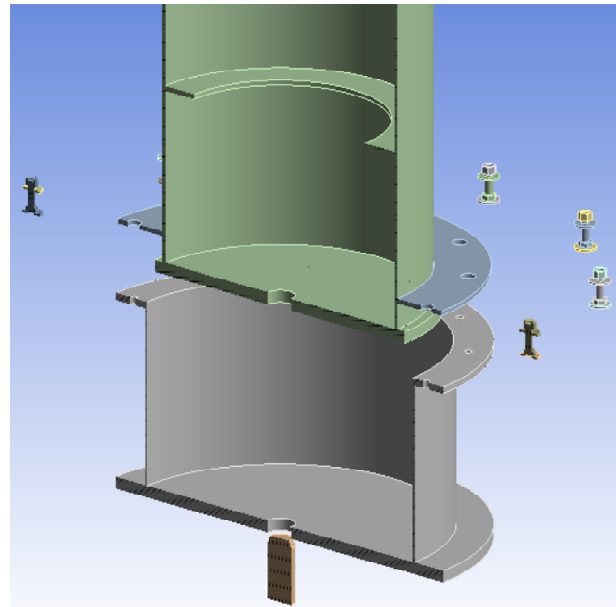


Figure 2. Rocking connection components.

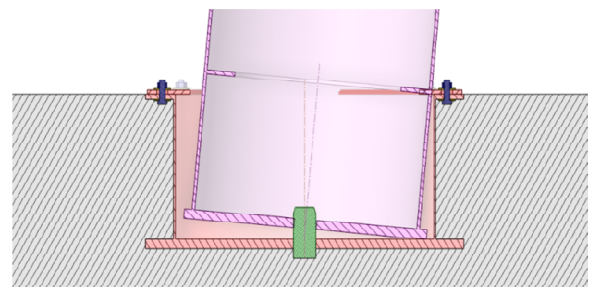
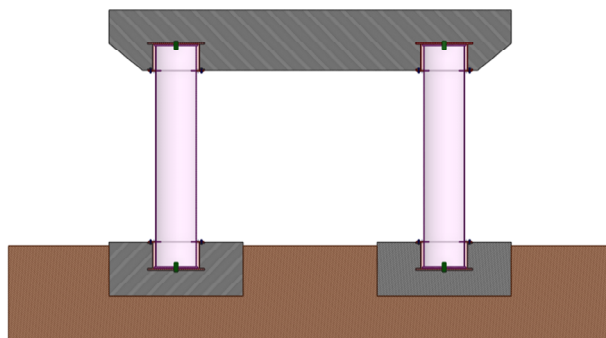
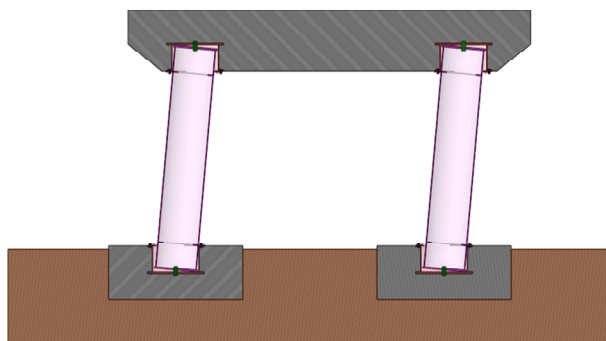


Figure 3. Pocket type rocking connection.



(a) Normal State



(b) Rocking State

Figure 1. Bridge bent with pocket type rocking connections - section view.

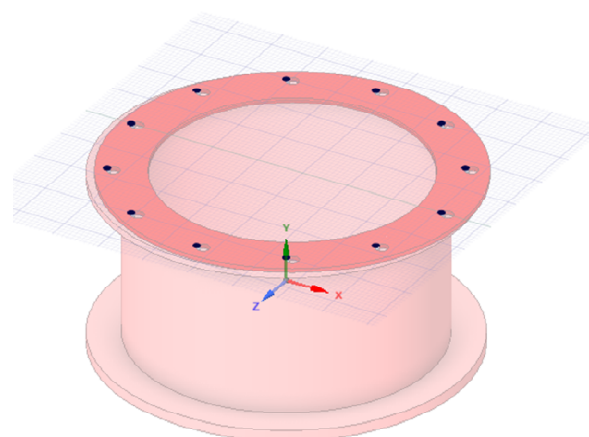


Figure 4. Position of ring plate during rocking.

sleeve component and the bolts during rocking. The ring plate shall be designed to yield and act as a fuse during large earthquakes and to remain essentially elastic during small and moderate earthquakes.

The lateral load transfer mechanism within the connection is similar to the back-span of a cantilever beam. The lateral load is transferred to the connection through the in-plane resistance of the ring plate, friction at the column tipping point, and the shear resistance of the shear pin. The prying action of the column would apply a substantial load on the ring plate and the shear pin, which can result in shear reversal, where the shear in the column changes direction within the connection.

4. Finite Element Analysis of Subassembly of a Typical Bridge Pier

The lateral response of the double-column bridge pier is similar to that of a subassembly comprising the lower portion of a column, as shown in Figure (5). Finite element analysis (FEA) was performed on the subassembly of a typical bridge pier. The subassembly consists of a 1220 mm-diameter tubular column with a 50 mm-thick end plate, a 1400 mm-diameter tubular sleeve with a top flange and an end plate, a 120 mm-diameter shear pin, and a 15 mm-thick ring plate, which is connected to the flange by twelve 30 mm high-strength bolts. The dimensions of the components are shown in Figure (6). All components are made of structural steel with a 350 MPa yield strength, except for the ring plate, which has a yield strength of 250 MPa.

4.1 Description of the FEA Model

The ANSYS finite element software was used to simulate the behavior of the subassembly under lateral cyclic loading. A cross-sectional view of the finite element model and the boundary conditions are shown in Figure (7). Fixed boundary condition was imposed on the embedded surfaces of the sleeve component, and gravity load and lateral displacement were applied on top of the sub-column. Solid elements with nonlinear material properties were used to model the column, the sleeve component, the ring plate, the shear pin, and

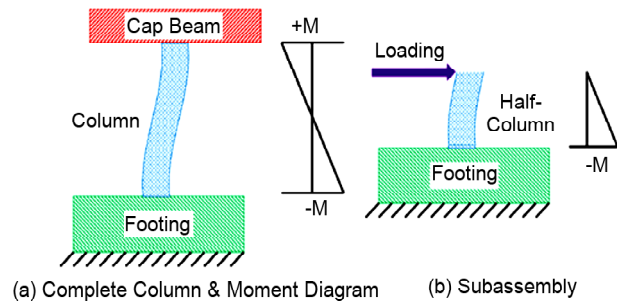


Figure 5. Schematics of the pier column and the corresponding subassembly.

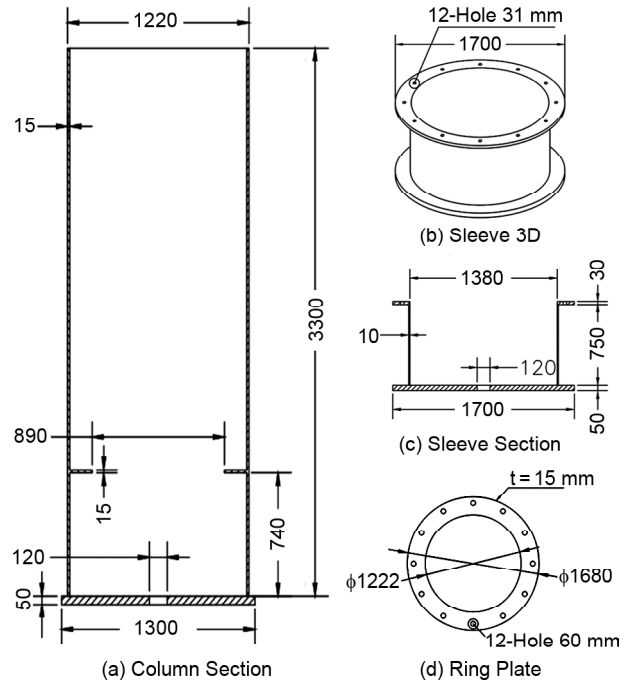


Figure 6. Typical plan and elevation views of the buildings.

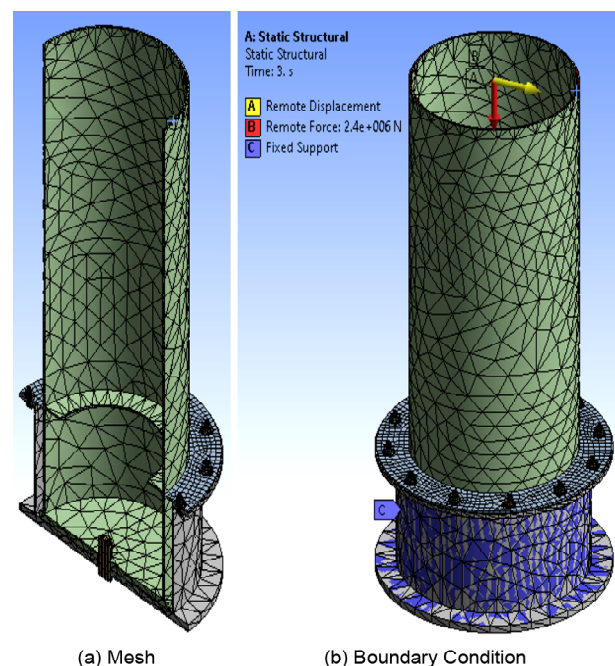


Figure 7. Finite element model of the subassembly.

the bolt assembly. The interaction between the components was modeled using contact elements at the contact interfaces. The contact interfaces included surfaces that were originally in contact or were expected to come into contact during the analysis. These surfaces include the contact areas associated with column and sleeve end plates, the shear pin and center holes of the end plates, the ring plate and sleeve flange, the ring plate and column wall, the ring plate and washers, and bolt shanks and boltholes in the ring plate and the flange. Friction-type surface-to-surface contacts with a friction coefficient of 0.2 were assigned at the contact surfaces.

Nonlinear static analyses were performed on the connection to evaluate the behavior of the connection under gravity and cyclic lateral loading. To evaluate the effect of gravity load on the hysteresis response of the connection, the analyses were performed for two gravity loads of 2400 kN and 1200 kN. Each analysis was carried out in several load steps. The gravity load was applied on top of the column in the first step, and a 300 kN preload was applied to each bolt during the second step. In the following load steps, cyclic lateral displacements (up to 4% drift ratio) were applied at the top of the column. To evaluate the response of the connection under free rocking condition, the analyses were repeated for the same gravity loads, but on a FE model that consisted of the column and the sleeve component without the ring plate, bolts, and shear pin. For the free rocking analyses, rough surface-to-surface contact, which allows for separation but not sliding, was used at the interface between the column and sleeve end plates.

4.2 Analyses Results

In this section, the results of the analysis under a gravity load of 2400 kN at 4% drift ratio are presented, and then the hysteresis responses of the subassembly under the two gravity loads are discussed. To illustrate the response of the contact elements during the lateral loading, the penetrations at the ring plate interfaces with the column and bolt shanks are shown in Figure (8) at 2.5% and 4% drifts. This figure shows that at the 2.5% drift, the ring plate is not contacting the bolt shanks, but

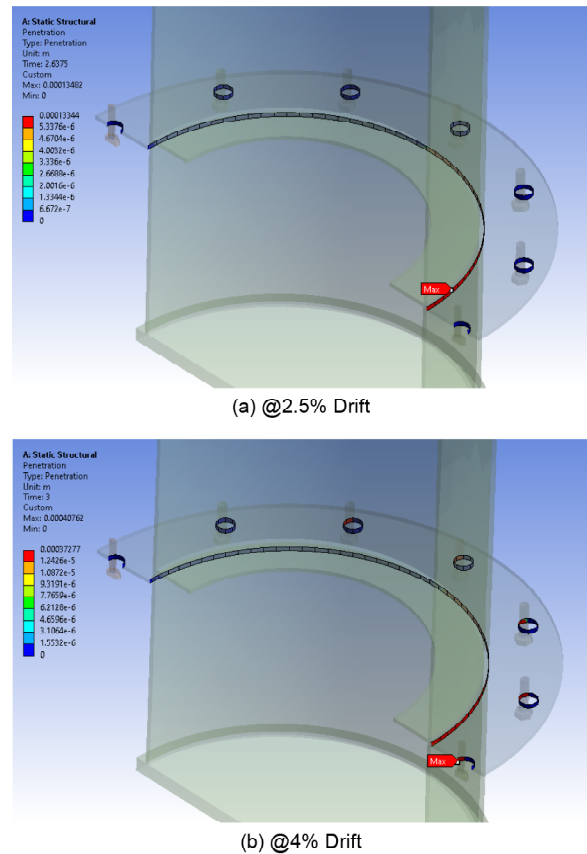


Figure 8. Contact penetration across ring plate interfaces with column and bolt shanks.

it is in contact with the leaning side of the column with a maximum penetration of 0.13 mm. At 4% drift, the ring plate is in contact with most of the bolts, with a maximum penetration of 0.37 mm at the bolthole located along the rocking plan. At this drift ratio, high contact pressures at boltholes lead to yielding and plastic deformation of the ring plate.

Figure (9) shows the equivalent (von-Mises) stress and equivalent plastic strain of the subassembly at 4% drift ratio. High local stresses occurred on the tipping side of the column, around the center boltholes, and on the column internal stiffener at 90 degrees from the rocking plane. The local high stress in the stiffener is due to the high pressure exerted by the ring plate on the column wall. The stresses in the ring plate are less than the maximum stress in the stiffener, mainly because of the lower yield strength of the ring plate. However, due to the lower yield strength, the ring plate is the primary component that experiences plastic deformations, as shown in Figure (9b).

Figure (10) shows the plastic strain distributions in the ring plate and the column at +/- 4% drift ratios.

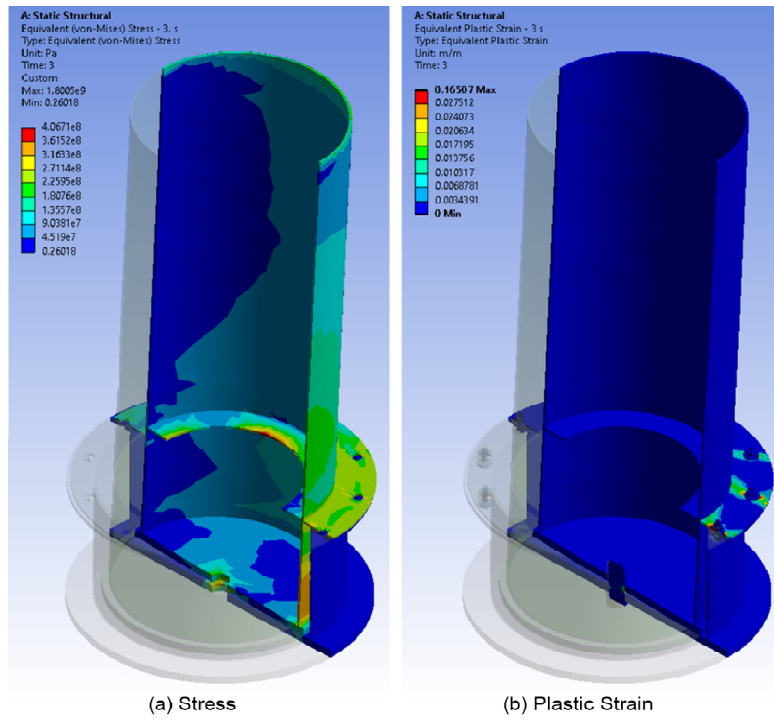


Figure 9. Equivalent stress and plastic strain at 4% drift ratio.

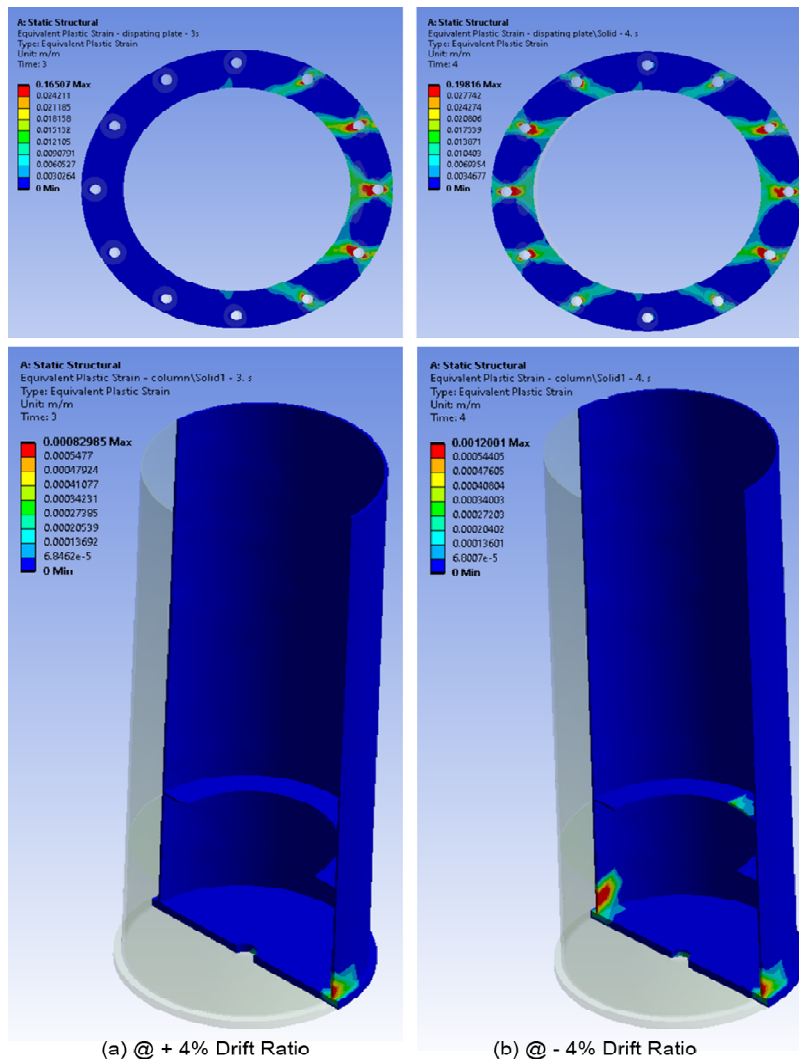


Figure 10. Plastic strain in ring plate and column at +/- 4% drift ratio.

This figure indicates extensive plastic deformation of the ring plate, with relatively high plastic strain near the boltholes after the loading cycle. It also indicates that the plastic deformation of the column is localized around the tipping point, the stiffener, and around the center pinhole. These results indicate that the ring plate is the primary component contributing to energy dissipation, initially through friction by sliding at the interface surface with the sleeve flange, and then by yielding of the plate.

Figure (11) shows the hysteresis response of the subassembly under the two gravity loads along with the free rocking cases. At a 4% drift ratio, the lateral resistance under gravity loads of 1200 kN and 2400 kN is, respectively, 730 kN and 920 kN. The loading curves of the subassembly show nearly constant lateral resistance in the 1%-2.6% drift range, followed by stiffening beyond 2.6% drift. For drift ratios less than 2.6%, the oversized boltholes in the ring plate remain disengaged from the pre-tensioned bolts, and the resistance provided by the ring plate is due to the friction between this plate and the sleeve flange. At the 2.6% drift ratio (Point A), the bolt shanks come into contact with the oversized holes in the ring plate, resulting in additional lateral resistance. During unloading, the ring plate initially separates from the bolt shanks and the column; hence, the unloading curves follow the free rocking curves up to the point where it re-engages with the column (Point B). At this stage, the frictional resistance at the plate-flange interface causes the unloading curves to deviate from

the free-rocking curves. The residual drift of the subassembly for gravity loads of 1200 kN and 2400 kN is 1.6% and 0.15%, respectively. The 1200 kN gravity load does not provide enough restoring force to overcome the frictional resistance at the plate-flange interface, and the corresponding unloading curve crosses the x-axis (zero lateral load) at relatively high drift ratio. On the other hand, the restoring force due to the 2400 kN gravity load exceeds the frictional resistance, and the unloading curve crosses the x-axis at a low drift ratio.

Any residual drift in the rocking connection can be recovered by loosening the preloaded bolts and removing the frictional resistance at the plate-flange interface. To demonstrate this point, an analysis of the subassembly with the 1200 kN gravity load was repeated with an additional load step at the residual drift of 1.6% (52 mm lateral displacement). During this load step, the bolt loads were gradually reduced (ramped unloading) while keeping the gravity load constant. The load-displacement behavior from this analysis is shown in Figure (12). It indicates that the residual displacement is recovered along a load path featuring stiffness reversals, as shown by the dashed curve. This curve intersects the x-axis at lateral displacements of 31 mm. At this point, the bolt loads are decreased by 35%. This indicates that the restoring force overcomes the frictional resistance when 35% of the bolt load is released, thereby enabling the connection to retain its upright position. These results show that the residual displacement of a bridge pier with this type of connection could be recovered by simply loosening

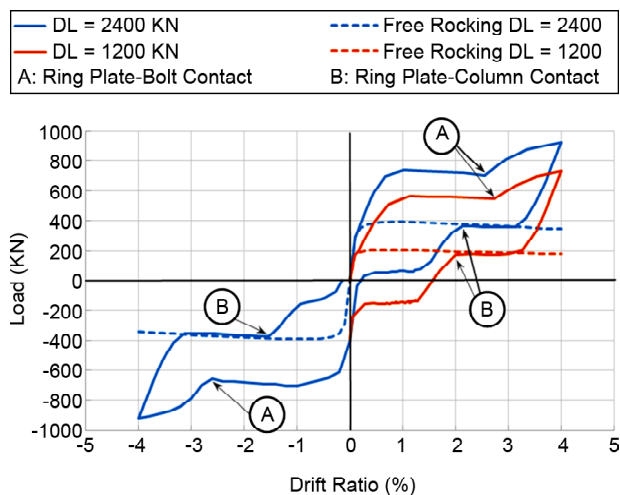


Figure 11. Lateral load vs. drift ratio.

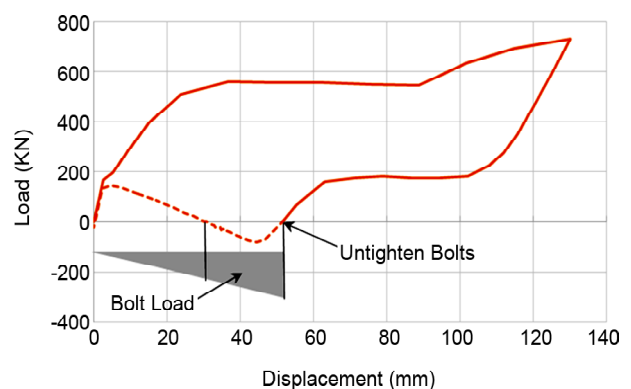


Figure 11. Lateral load vs. displacement for 1200 kN gravity load.

the bolts in each connection. This action would diminish the frictional resistance of the connection and would allow the pier to be restored to its upright position by the gravity load.

The results of the analyses indicate that the rocking connection provides satisfactory lateral resistance with a flag-shaped hysteresis response with marginal or recoverable residual displacements. These results indicate that the ring plate is the primary component contributing to energy dissipation, initially through friction by sliding against the sleeve flange, and then by yielding of the plate. This simple and practical connection improves the seismic performance of bridges. The recoverability of the residual drift after a seismic event by simply untightening the bolts in each connection makes it an attractive option for bridge design.

5. Summary and Conclusions

The study introduces a novel rocking system designed to enhance the seismic performance of bridges. The bridge bent in this system consists of a precast cap beam, a pair of prefabricated tubular steel columns, and pocket-type rocking connections. The rocking connection consists of an embedded steel sleeve component designed to receive the column end, a center shear pin, and a ring plate bearing against the column and connected to the sleeve component by high-strength bolts. The boltholes in the ring plate are oversized to allow for sliding relative to the embedded sleeve component. During rocking, the ring plate provides two-level energy dissipation: initially through friction at low and moderate drifts and subsequently through material yielding at high drifts. This system does not utilize post-tensioned tendons and relies solely on gravity for re-centering.

A finite element model was developed to simulate the complex response of the multipart connection, which includes the column, the embedded sleeve, the ring plate, the shear pin, and the bolt assembly. Solid elements with nonlinear material properties were used to model each component, and contact elements were used to simulate the behavior of surfaces in contact with one another. Nonlinear static analyses under gravity and cyclic lateral loading were performed on the subassembly of a typical bridge pier. The subassembly consisted of

the lower half of a column and its associated rocking connection. The analyses were performed for two gravity loads to evaluate the effect of the gravity load on the hysteresis response. In order to evaluate the response of the subassembly under free rocking conditions, the analyses were repeated for the same gravity loads, but on a separate FE model that consisted of the column and the sleeve component without the ring plate, bolts, and shear pin. In this particular model, rough contact elements that allow for separation but not sliding were used at the rocking interface.

The results of the finite element analyses (FEA) indicate that the rocking system provides satisfactory lateral resistance with a flag-shaped hysteresis response with marginal or recoverable residual displacements. These results indicate that the ring plate is the primary component contributing to energy dissipation, initially through friction by sliding against the sleeve flange, and then by yielding of the plate. The FEA results showed that the re-centering characteristic of the system is dependent on the restoring force of the gravity load and the frictional resistance of the rocking connection. If the restoring force exceeds the frictional resistance, full re-centering of the system would be achieved. However, if the restoring force fails to overcome the frictional resistance, partial re-centering would occur, along with some residual displacement. The FEA also demonstrated that any residual displacement within this system could be recovered by merely untightening the bolts in the connection. The ability to recover the residual drift by simply loosening the bolts after a seismic event is a remarkable and appealing feature of this system.

References

- Aoki, T., & Susantha, K.A.S. (2005). Seismic Performance of rectangular-shaped steel piers under cyclic loading. *Journal of Structural Engineering*, 131(2), 240-249. [https://doi.org/10.1061/\(asce\)0733-9445\(2005\)131:2\(240\)](https://doi.org/10.1061/(asce)0733-9445(2005)131:2(240)).
- Association, J.R. (2002). *Design Specifications of Highway Bridges, Part V Seismic Design*. Maruzen, Tokyo, Japan.
- Aydan, O. (2008). A reconnaissance report on

2008 Wenchuan earthquake.

Billington, S.L., & Yoon, J.K. (2004). Cyclic response of unbonded posttensioned precast columns with ductile fiber-reinforced concrete. *Journal of Bridge Engineering*, 9(4), 353-363. [https://doi.org/10.1061/\(asce\)1084-0702\(2004\)9:4\(353\)](https://doi.org/10.1061/(asce)1084-0702(2004)9:4(353)).

Bozorgnia, Y., & Bertero, V.V. (2004). *Earthquake Engineering: From Engineering Seismology to Performance-Based Engineering*. CRC press.

Bruneau, M., Wilson, J.C., & Tremblay, R. (1996). Performance of steel bridges during the 1995 Hyogo-ken Nanbu (Kobe, Japan) earthquake. *Canadian Journal of Civil Engineering*, 23(3), 678-713. <https://doi.org/10.1139/196-883>.

Cheok, G.S., & Lew, H.S. (1991). Performance of Precast Concrete Beam-to-Column Connections Subject to Cyclic Loading. *PCI Journal*, 36(3), 56-67. <https://doi.org/10.15554/pcij.05011991.56.67>.

Christopoulos, C., Filiatrault, A., Uang, C.-M., & Folz, B. (2002). Posttensioned energy dissipating connections for moment-resisting steel frames. *Journal of Structural Engineering*, 128(9), 1111-1120. [https://doi.org/10.1061/\(asce\)0733-9445\(2002\)128:9\(1111\)](https://doi.org/10.1061/(asce)0733-9445(2002)128:9(1111)).

Christopoulos, C., Tremblay, R., Kim, H.J., & Lacerte, M. (2008). Self-centering energy dissipative bracing system for the seismic resistance of structures: development and validation. *Journal of Structural Engineering*, 134(1), 96-107. [https://doi.org/10.1061/\(asce\)0733-9445\(2008\)134:1\(96\)](https://doi.org/10.1061/(asce)0733-9445(2008)134:1(96)).

Culmo, M.P., Lord, B., Huie, M., & Beerman, B. (2011). Accelerated bridge construction: Experience in design, fabrication and erection of prefabricated bridge elements and systems: Final manual.

ElGawady, M.A., & Sha'lan, A. (2011). Seismic behavior of self-centering precast segmental bridge bents. *Journal of Bridge Engineering*, 16(3), 328-339. [https://doi.org/10.1061/\(asce\)be.1943-5592.0000174](https://doi.org/10.1061/(asce)be.1943-5592.0000174).

Elnashai, A.S., Gencturk, B., Kwon, O.-S., Hashash, Y.M.A., Kim, S.J., Jeong, S.-H., & Dukes, J. (2012). The Maule (Chile) earthquake of February 27, 2010: Development of hazard, site specific ground motions

and back-analysis of structures. *Soil Dynamics and Earthquake Engineering*, 42, 229-245. <https://doi.org/10.1016/j.soildyn.2012.06.010>.

Ge, H., Kang, L., & Tsumura, Y. (2013). Extremely low-cycle fatigue tests of thick-walled steel bridge piers. *Journal of Bridge Engineering*, 18(9), 858-870. [https://doi.org/10.1061/\(asce\)be.1943-5592.0000429](https://doi.org/10.1061/(asce)be.1943-5592.0000429).

Guerrini, G., Restrepo, J.I., Massari, M., & Vervelidis, A. (2015). Seismic behavior of posttensioned self-centering precast concrete dual-shell steel columns. *Journal of Structural Engineering*, 141(4). [https://doi.org/10.1061/\(asce\)st.1943-541x.0001054](https://doi.org/10.1061/(asce)st.1943-541x.0001054).

Hewes, J.T. (2002). *Seismic Design and Performance of Precast Concrete Segmental Bridge Columns*. University of California, San Diego.

Housner, G.W. (1963). The behavior of inverted pendulum structures during earthquakes. *Bulletin of the Seismological Society of America*, 53(2), 403-417. <https://doi.org/10.1785/bssa0530020403>.

Li, L., Mander, J.B., & Dhakal, R.P. (2008). Bidirectional cyclic loading experiment on a 3D beam-column joint designed for damage avoidance. *Journal of Structural Engineering*, 134(11), 1733-1742. [https://doi.org/10.1061/\(asce\)0733-9445\(2008\)134:11\(1733\)](https://doi.org/10.1061/(asce)0733-9445(2008)134:11(1733)).

MacRae, G.A., & Kawashima, K. (2001). Seismic behavior of hollow stiffened steel bridge columns. *Journal of Bridge Engineering*, 6(2), 110-119. [https://doi.org/10.1061/\(asce\)1084-0702\(2001\)6:2\(110\)](https://doi.org/10.1061/(asce)1084-0702(2001)6:2(110)).

Mander, J., & Cheng, C. (1997). *Seismic Resistance of Bridge Piers Based on Damage Avoidance Design*. Technical Report CEER-97-0014.

Nishikawa, K., Yamamoto, S., Natori, T., Terao, O., Yasunami, H., & Terada, M. (1996). An experimental study on improvement of seismic performance of existing steel bridge piers. *Journal of Structural Engineering, JSCE*, 42(3), 975-986.

Palermo, A., Pampanin, S., & Marriott, D. (2007). Design, Modeling, and Experimental Response of Seismic Resistant Bridge Piers with Posttensioned

- Dissipating Connections. *Journal of Structural Engineering*, 133(11), 1648-1661. [https://doi.org/10.1061/\(asce\)0733-9445\(2007\)133:11\(1648\)](https://doi.org/10.1061/(asce)0733-9445(2007)133:11(1648)).
- Priestley, M.J.N., & Tao, J.R. (1993). Seismic response of precast prestressed concrete frames with partially debonded tendons. *PCI Journal*, 38(1), 58-69. <https://doi.org/10.15554/pcij.01011993>. 58.69.
- Ricles, J.M., Sause, R., Garlock, M.M., & Zhao, C. (2001). Posttensioned seismic-resistant connections for steel frames. *Journal of Structural Engineering*, 127(2), 113-121. [https://doi.org/10.1061/\(asce\)0733-9445\(2001\)127:2\(113\)](https://doi.org/10.1061/(asce)0733-9445(2001)127:2(113)).
- Ricles, J.M., Sause, R., Peng, S.W., & Lu, L.W. (2002). Experimental evaluation of earthquake resistant posttensioned steel connections. *Journal of Structural Engineering*, 128(7), 850-859. [https://doi.org/10.1061/\(asce\)0733-9445\(2002\)128:7\(850\)](https://doi.org/10.1061/(asce)0733-9445(2002)128:7(850)).
- Rodgers, G.W., Solberg, K.M., Mander, J.B., Chase, J.G., Bradley, B.A., & Dhakal, R.P. (2012). High-force-to-volume seismic dissipators embedded in a jointed precast concrete frame. *Journal of Structural Engineering*, 138(3), 375-386. [https://doi.org/10.1061/\(asce\)st.1943-541x.0000329](https://doi.org/10.1061/(asce)st.1943-541x.0000329).
- Solberg, K., Mashiko, N., Mander, J.B., & Dhakal, R.P. (2009). Performance of a damage-protected highway bridge pier subjected to bidirectional earthquake attack. *Journal of Structural Engineering*, 135(5), 469-478. [https://doi.org/10.1061/\(asce\)0733-9445\(2009\)135:5\(469\)](https://doi.org/10.1061/(asce)0733-9445(2009)135:5(469)).
- Stone, W.C., Cheok, G.S., & Stanton, J.F. (1995). Performance of hybrid moment-resisting precast beam-column concrete connections subjected to cyclic loading. *ACI Structural Journal*, 92(2). <https://doi.org/10.14359/1145>.
- Susantha, K.A.S., Aoki, T., & Kumano, T. (2006). Strength and ductility evaluation of steel bridge piers with linearly tapered plates. *Journal of Constructional Steel Research*, 62(9), 906-916. <https://doi.org/10.1016/j.jcsr.2005.11.006>.
- Thonstad, T., Kennedy, B.J., Schaefer, J.A., Eberhard, M.O., & Stanton, J.F. (2017). Cyclic tests of precast pretensioned rocking bridge-column subassemblies. *Journal of Structural Engineering*, 143(9). [https://doi.org/10.1061/\(asce\)st.1943-541x.0001823](https://doi.org/10.1061/(asce)st.1943-541x.0001823).
- Tremblay, R., Lacerte, M., & Christopoulos, C. (2008). Seismic response of multistory buildings with self-centering energy dissipative steel braces. *Journal of Structural Engineering*, 134(1), 108-120. [https://doi.org/10.1061/\(asce\)0733-9445\(2008\)134:1\(108\)](https://doi.org/10.1061/(asce)0733-9445(2008)134:1(108)).
- Trono, W., Jen, G., Panagiotou, M., Schoettler, M., & Ostertag, C.P. (2015). Seismic response of a damage-resistant recentering posttensioned-HYFRC Bridge Column. *Journal of Bridge Engineering*, 20(7). [https://doi.org/10.1061/\(asce\)be.1943-5592.0000692](https://doi.org/10.1061/(asce)be.1943-5592.0000692).
- Vasdravellis, G., Karavasilis, T.L., & Uy, B. (2013). Large-scale experimental validation of steel posttensioned connections with web hourglass Pins. *Journal of Structural Engineering*, 139(6), 1033-1042. [https://doi.org/10.1061/\(asce\)st.1943-541x.0000696](https://doi.org/10.1061/(asce)st.1943-541x.0000696).
- Vasseghi, A., & Mahmoudi, M.H. (2024). Development of a novel rocking connection for tubular steel bridge piers: A proof of concept study. *Earthquake Engineering & Structural Dynamics*. <https://doi.org/10.1002/eqe.4185>.
- Vasseghi, A., Mansouri, B., & Rointan, S. (2021). Feasibility study on utilizing self-centering structural system for typical highway bridges in Iran. *Amirkabir Journal of Civil Engineering*, 53(10), 4359-4378. <https://doi.org/10.22060/ceej.2020.18323.6835>.
- White, S., & Palermo, A. (2016). Quasi-static testing of posttensioned nonemulative column-footing connections for bridge piers. *Journal of Bridge Engineering*, 21(6). [https://doi.org/10.1061/\(asce\)be.1943-5592.0000872](https://doi.org/10.1061/(asce)be.1943-5592.0000872).
- Wolski, M., Ricles, J.M., & Sause, R. (2009). Experimental study of a self-centering beam-column connection with bottom flange friction device. *Journal of Structural Engineering*, 135(5), 479-488. [https://doi.org/10.1061/\(asce\)st.1943-541x.0000006](https://doi.org/10.1061/(asce)st.1943-541x.0000006).